

# Non-Destructive Evaluation of FSW Tool Plunge Depth in Thin Metallic Sheet Weld Using Ultrasonic Guided Waves

---

MANISH KUMAR MEHTA, GOVINDA GAUTAM,  
D. M. JOGLEKAR and D. K. DWIVEDI

## ABSTRACT

Due to their high strength-to-weight ratio, thin aluminium alloy sheets are widely used in industries such as automotive, marine, railway, and aerospace. Welding has been discovered to be an effective method of joining, particularly in comparison to mechanical fasteners and semi-joining processes. However, fusion welding techniques can be vulnerable to hot cracking, which can result in solidification and liquation cracking. For lap welded joints in thin metallic sheets, friction stir welding (FSW) has proven to be very efficient. Non-destructive testing (NDT) methods are utilized to examine weld morphology. The ultrasonic method has demonstrated the ability to measure weld penetration depth in thick metallic plates using bulk and surface waves. However, the tool plunge depth (TPD) in FSW, which is analogous to the weld penetration depth of fusion welding, plays a crucial role in the weld strength of thin structures that has not been investigated using non-destructive methods. This study aimed to predict the optimum tool plunge depth for sound welding in thin structures by employing a guided Lamb wave-based non-destructive method. At a low frequency of 25kHz, only anti-symmetric (Ao) mode was transmitted through low TPD weld and through optimum TPD weld both Ao and symmetric mode (So) was getting transmitted. However, through high TPD weld both Ao and So was getting transmitted as well as extra anti-symmetric (AoAoc or SoAoc) mode was observed due to mode conversion. This different scattering behaviour of Lamb wave signals for varying tool plunge depths was analysed to predict the FSW tool plunge depths with accuracy.

## INTRODUCTION

The automotive, aerospace, and marine industries are experiencing a significant rise in the utilization of high-strength steels and aluminium to achieve weight reduction in various components. There is growing research interest in the joining technology of different materials. Steel together with Al alloy is considered the most important dissimilar material combination, for which various approaches have been investigated. Friction stir welding (FSW) is an innovative welding method that employs traditionally challenging to weld using fusion welding methods [1].

---

Manish Kumar Mehta<sup>1</sup>, Govinda Gautam<sup>1</sup>, D. M. Joglekar<sup>1</sup>, D. K. Dwivedi<sup>1</sup>.

<sup>1</sup> Department of Mechanical and Industrial Engineering, Indian Institute of Technology Roorkee, 247667 Roorkee, Uttarakhand, India

There is no bulk material melting in FSW, since welding is carried at a lesser temperature than melting points of the joined metals. Hence mechanical properties of weld improves which serves advantage over other welding methods. Friction Stir Welding is a welding technique that has a limited number of process parameters that can be controlled to produce high-quality welds. The parameters encompass tool rotational speed, tool traverse feed, axial load, plunge depth, tool geometry, and tool tilt angle. One of the critical parameters that affect weld quality is the Tool Plunge Depth (TPD), which directly impacts the strength of the welded parts. To determine the TPD, traditional methods involve cutting and checking the welded parts, which is a costly and inefficient process. However, Non-destructive Evaluation (NDE) provides a more practical solution for testing the quality of thin sheet metal welds without damaging the parts during the inspection process. Among the various NDE techniques available, Ultrasonic Testing (UT) is the preferred method for welded components. UT has the capability to detect and size both planar and volumetric defects in the welded parts.

Numerous non-destructive testing techniques have been developed for assessing the quality of welds [2]. These techniques include visual inspection, infrared thermography method, magnetic particle inspection, liquid penetrant inspection, eddy current inspection, traditional ultrasonic testing, and others [3-6]. Researchers have explored the use of these techniques to improve the evaluation of FSW joints. For instance, Tarraf et al. studied the scattering behaviour of guided waves in similar and dissimilar FSW joints to determine the elastic properties of the joint in thick plates [7]. Fakih et al. used advanced signal processing techniques to detect defects in FSW joints in thick sheets [8]. Wang et al. used guided wave propagation to investigate the impact of concave cross-sectional shape and different microstructure-mechanical parameters in thick plate FSW joints [9]. However, NDE of FSW joints in thin metal sheets is an area with limited literature available. Moreover, there is a lack of studies that quantify the tool plunge depth in FSW joints using non-destructive methods. To address this research gap, an experimental analysis was conducted to investigate the guided wave scattering behaviour in FSW joints of thin metallic sheets. The ultimate goal of this analysis is to predict the optimum TPD among lap welds of different TPD specimens.

## **TOOL PLUNGE DEPTH (TPD)**

In Friction Stir Welding, Tool Plunge Depth (TPD) is defined as the depth of the lowest point of the shoulder below the surface of the welded plate (as shown in Figure 1), and it is a critical parameter for heat generation and proper material joining without defects. The depth of plunge affects velocity of material flow and defect formation in stir zone. In lap weld low TPD results in incomplete mixing of skin and flange, while high TPD causes surface flash. An excessive TPD increases frictional heat and axial force, which hinders the mixing of skin and flange. Therefore, optimizing TPD to achieve the best material flow and avoid void formation for good mechanical properties is crucial.

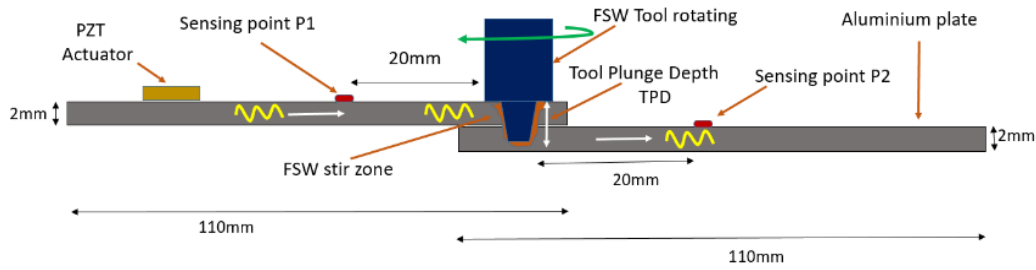


Figure 1. FSW specimen showing tool plunge depth (TPD), PZT actuator, sensing points P1, P2.

## SAMPLE PREPARATION

Friction Stir Welding (FSW) was used to join 2mm thick 6061 Al alloy sheets with high carbon high chromium steel (HcHcr) in this study. For the welding process, a Computer Numerical Control (CNC) FSW machine was utilized, and raw materials were cut from an Al-6061 aluminium alloy sheet. The dimensions of the prepared specimens were 110 mm  $\times$  240 mm  $\times$  2 mm for the skin and 110 mm  $\times$  240 mm  $\times$  2 mm for the flange. The elastic properties of the materials used were density ( $\rho$ ) = 2680 kg/m<sup>3</sup>, Young's modulus ( $E$ ) = 70.3 GPa, and Poisson's ratio ( $\nu$ ) = 0.33. The FSW parameters used during welding included a tool rpm of 1200, pin tilt angle of 2°, weld penetration depth of 3.6mm, and transverse speed of 75 mm/min. Various specimens were made with different plunging depths (3.36 mm, 3.66 mm, and 3.86 mm) by varying the tool plunge depth (as shown in Figure 2).

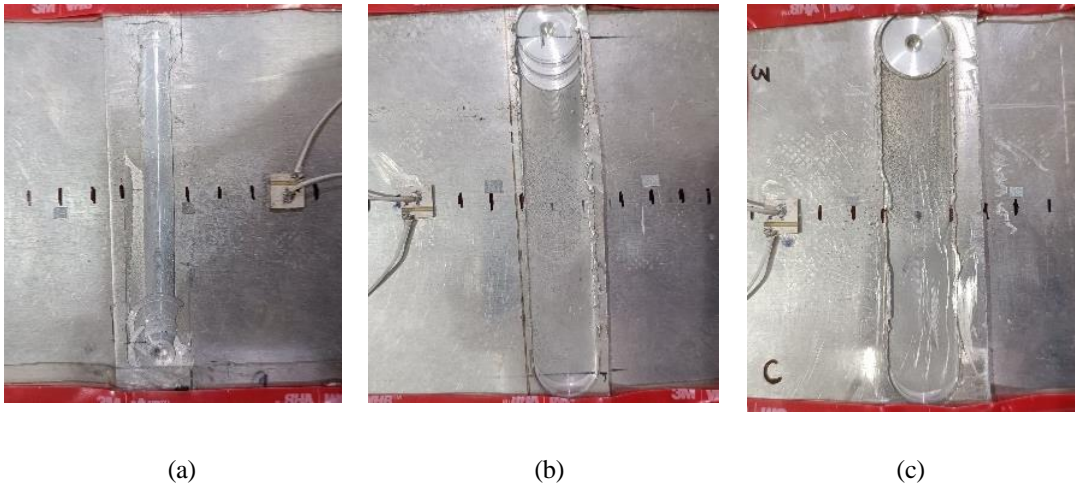


Figure 2. FSW samples used for the investigation (a) Low TPD of 3.36 mm; (b) Optimum TPD of 3.66 mm; (c) High TPD of 3.86 mm.

## EXPERIMENTAL SET-UP

Piezo-electric transducers (PZTs) of SP-5H type were used as an actuator to generate Lamb waves in the specimen [10]. These transducers are small, lightweight, and relatively low-cost, known for their strain-coupled transducer qualities. To attach the  $10 \times 10 \text{ mm}^2$  and 1 mm thick PZTs onto the plate surface, phenyl salicylate was used, and they were positioned 40 mm behind the weld zone. PZTs can convert electrical energy into acoustic energy, which generates Lamb waves within the structural material via ultrasonic wave propagation when an electric current is applied. The experimental set-up (illustrated in Figure 3) included a single-point Laser Doppler Vibrometer (Polytec Inc.), which had a laser unit for scanning out-of-plane displacement, an in-built function generator, and a data acquisition system. A bipolar voltage amplifier was utilized to amplify the voltage signal generated from the function generator. The voltage signal was amplified from 6 Vpp (Voltage peak to peak) to 60 Vpp. To generate the Lamb wave signal, a longitudinal force was applied using a four-cycle 25 kHz Hanning windowed tone burst, as shown in Figure 4. The waves were produced from the PZT location and spread throughout the lateral plane of the welded plate. Viscous damping tape was applied to the outer edge of the welded plate to prevent unnecessary noise and signal reflections from the free edge boundary. The Lamb wave signal was then detected by a laser head in a pitch-catch arrangement (as shown in Figure 1) at sensing points P1 and P2 as it passed through the weld zone. P1 was located 20 mm behind the lap weld zone, and P2 was located 20 mm after the weld zone. These steps of actuation, sensing, and signal data acquisition were repeated for all three specimens with different weld penetration depths. Finally, the displacement vs. time output data (signal) was further analysed.

## RESULTS AND DISCUSSION

When a force of 25 kHz as input frequency (Figure 4) was applied to the specimen through PZT, it was observed that two wave packets were generated. The group velocity of both packets was calculated experimentally and compared with the values obtained from the dispersion curve obtained numerically using the semi-analytical finite element

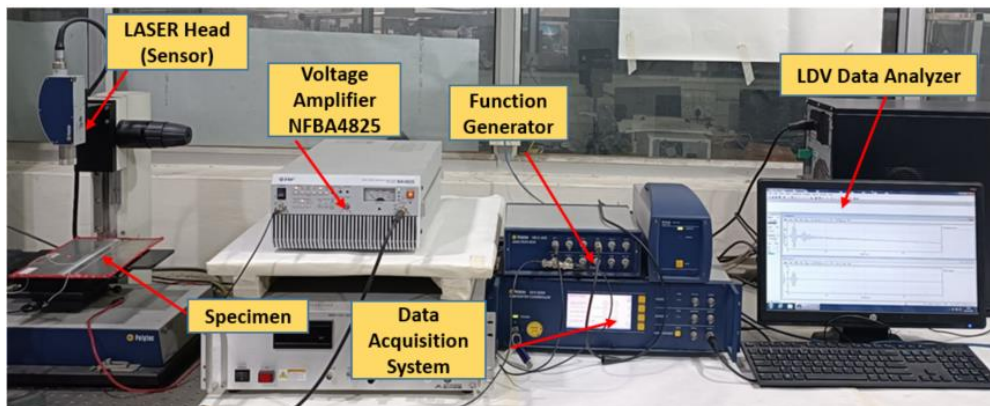
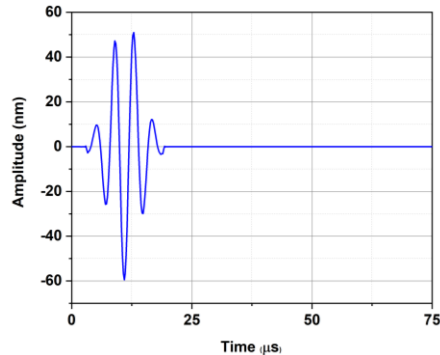
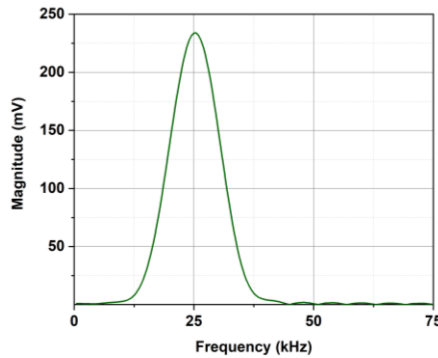


Figure 3. Experimental set-up

(SAFE) code in MATLAB (shown in Figure 7). One of these wave packets was identified as the fundamental anti-symmetric mode (Ao) while the other was the fundamental symmetric mode (So). Therefore, when the guided wave was initially produced at 25 kHz, it contained both Ao and So mode as shown in Figure 5. The scattering behavior of the Lamb wave passing through the FSW stir zone was different for different plunge depth specimens. The guided wave, consisting of both the anti-symmetric (Ao) and symmetric (So) modes, was found to behave differently when passing through FSW specimens with varying tool plunge depths. In specimens with low TPD, a significant portion of the So mode was reflected back, with only a small amount transmitted from the top sheet to the bottom sheet as shown in Figure 6 (a). However, a good percentage of the Ao mode was transmitted. In contrast, in specimens with optimum TPD, both Ao and So modes were strongly transmitted as shown in Figure 6 (b). But in FSW specimen with excessive or higher TPD, both Ao and So modes were strongly transmitted as well as a new lobe was observed, which was calculated to be the anti-symmetric mode generated due to mode conversions (AoAoc or SoAoc) from the initially propagating Ao or So modes as shown in Figure 6 (c). To verify the modes of these wave packets, their group velocity was calculated experimentally and compared with values obtained numerically from the dispersion curve obtained using semi-analytical finite element (SAFE) code in MATLAB as shown in Figure 7.



(a)



(b)

Figure 4. Four periods of 25 kHz Hanning windowed tone burst input signal in (a) time domain; (b) frequency domain

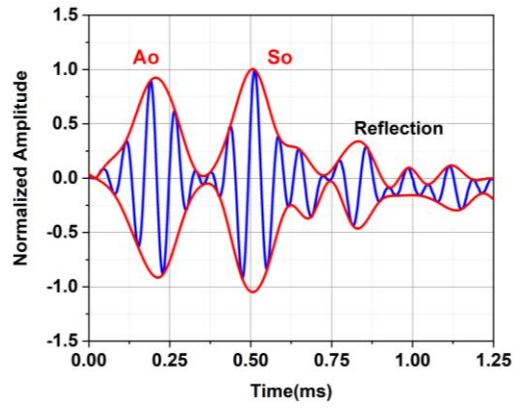
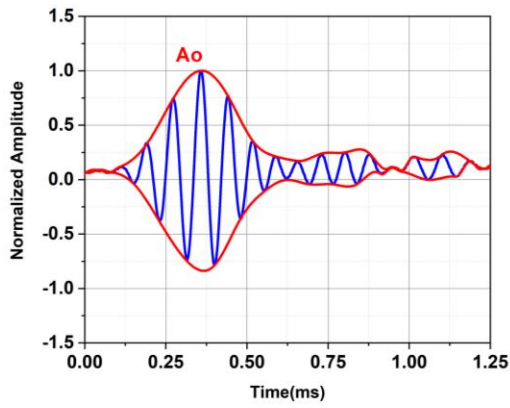
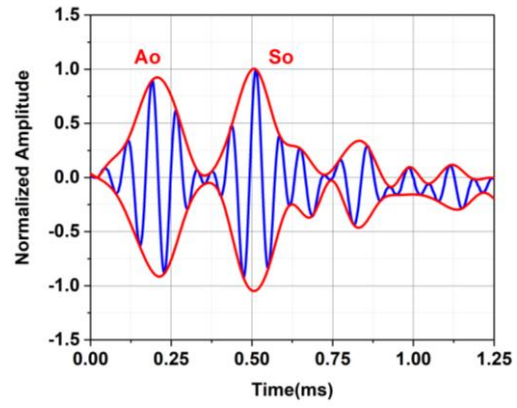


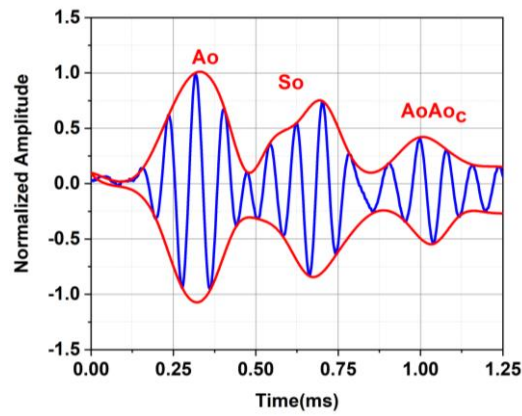
Figure 5. Guided wave signal sensed at a distance of 20mm before FSW weld zone in low, high, optimum tool plunge depths specimens (identical signals in all specimens)



(a)



(b)



(c)

Figure 6. Guided wave signal sensed at distance of 20mm after FSW weld zone in: (a) low; (b) optimum; (c) high plunge depths specimens.



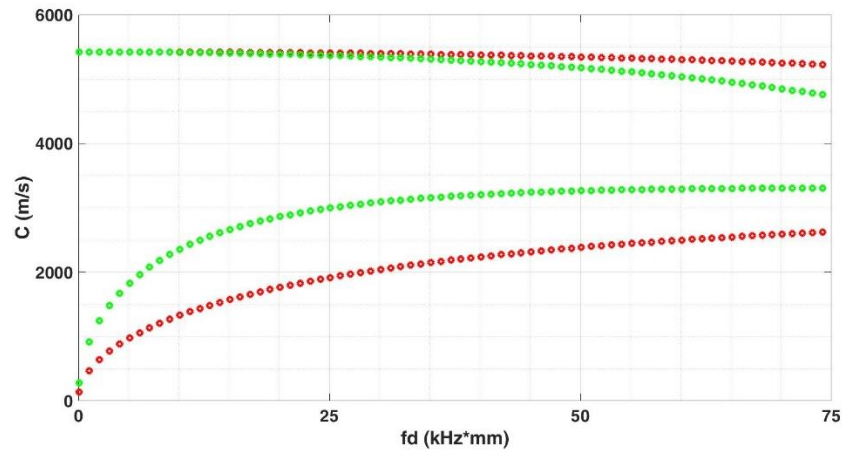


Figure 7. Lamb waves phase (red) and group (green) velocities dispersion curves for 2mm thickness 6061- aluminum alloy plate.

### DESTRUCTIVE TESTING METHOD: CUT-CHECK AND TENSILE TEST

Plunge depth characterization involved destructive testing methods such as stereoscopy and tensile testing. For stereoscopy analysis, ASTM standard samples were manufactured using a wire EDM CNC cutting machine and were subsequently diamond polished for further characterization. The stereoscopy images, along with plunge depth measurements, can be seen in Figure 8. To conduct the tensile testing, the welded joints were sliced perpendicularly to the direction of the weld using a wire EDM CNC cutting machine, following the dimensions specified in ASTM guidelines to obtain the required tensile specimens. It was observed that the formation of the joint and the mechanical properties were significantly affected by the plunge depth. A relatively low plunge depth of 3.36 mm led to insufficient root penetration and reduced tensile load carrying capacity. Conversely, a high plunge depth of 3.86 mm resulted in stress concentration and severe softening. The optimum plunge depth of 3.66 mm was determined to achieve the highest maximum tensile load carrying capacity (as shown in Figure 8).

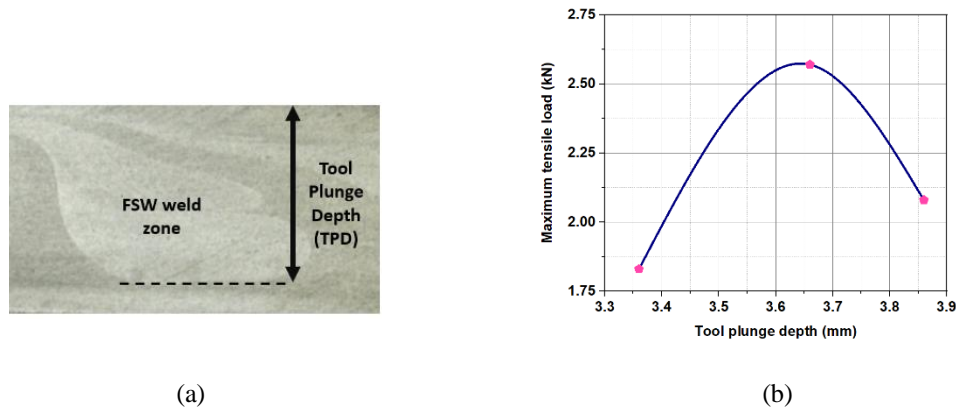


Figure 8. Destructive testing results for: (a) Stereoscopy image of FSW stir zone; (b) Maximum tensile load versus tool plunge depth

## CONCLUSIONS

The optimal tool plunge depth is predicted for achieving high-quality welding in thin structures using a non-destructive method based on the ultrasonic guided Lamb waves. Various welded specimens were examined, including those with lower, optimum, and higher tool plunge depths. At a low frequency of 25 kHz, both the fundamental symmetric (So) and antisymmetric (Ao) modes were excited by a PZT transducer and propagated through the entire thin sheet specimen. Through the low tool plunge depth weld, only the anti-symmetric (Ao) mode was transmitted, while through the optimum tool plunge depth weld, both the Ao and So modes were successfully transmitted. However, in the high tool plunge depth weld, both the Ao and So modes were transmitted, along with the observation of additional anti-symmetric (AoAoc or SoAoc) mode generation due to mode conversion. These findings demonstrate that different tool plunge depths exhibit distinct behaviours in guided Lamb wave propagation, allowing for accurate prediction of the tool plunge depths in friction stir welded joints.

## REFERENCES

1. Taban, E., Gould, J. E., & Lippold, J. C. (2010). Dissimilar friction welding of 6061-T6 aluminum and AISI 1018 steel: Properties and microstructural characterization. *Materials & Design (1980-2015)*, 31(5), 2305-2311.
2. Gangwar, A. S., Agrawal, Y., & Joglekar, D. M. (2021). Nonlinear interactions of lamb waves with a delamination in composite laminates. *Journal of Nondestructive Evaluation, Diagnostics and Prognostics of Engineering Systems*, 4(3).
3. Bagavathiappan, S., Lahiri, B. B., Saravanan, T., Philip, J., & Jayakumar, T. (2013). Infrared thermography for condition monitoring—A review. *Infrared Physics & Technology*, 60, 35-55.
4. Lovejoy, M. J. (1993). *Magnetic particle inspection: a practical guide*. Springer Science & Business Media.
5. Park, D. G., Angani, C. S., Rao, B. P. C., Vértesy, G., Lee, D. H., & Kim, K. H. (2013). Detection of the subsurface cracks in a stainless steel plate using pulsed eddy current. *Journal of Nondestructive Evaluation*, 32, 350-353.
6. Mitra, A. K., Aradhye, A. A., & Joglekar, D. M. (2023). Low frequency ultrasonic guided wave propagation through honeycomb sandwich structures with non-uniform core thickness. *Mechanical Systems and Signal Processing*, 191, 110155.
7. Tarraf, J., Mustapha, S., Fakihi, M. A., Harb, M., Wang, H., Ayoub, G., & Hamade, R. (2018). Application of ultrasonic waves towards the inspection of similar and dissimilar friction stir welded joints. *Journal of Materials Processing Technology*, 255, 570-583.
8. Fakihi, M. A., Mustapha, S., Tarraf, J., Ayoub, G., & Hamade, R. (2018). Detection and assessment of flaws in friction stir welded joints using ultrasonic guided waves: experimental and finite element analysis. *Mechanical Systems and Signal Processing*, 101, 516-534.
9. Wang, Y., Gao, T., Liu, D., Sun, H., Miao, B., & Qing, X. (2020). Propagation characteristics of ultrasonic weld-guided waves in friction stir welding joint of same material. *Ultrasonics*, 102, 106058.
10. Agrawal, Y., Gangwar, A. S., & Joglekar, D. M. (2022). Localization of a breathing delamination using nonlinear lamb wave mixing. *Journal of Nondestructive Evaluation, Diagnostics and Prognostics of Engineering Systems*, 5(3), 031005.